Othman N., Kanazaki M., Abd. Wahid M., Mat S., Mohd Jaafar M.N., Wan Omar W.Z., Mansor S., Dahalan M.N., Mohd Nasir M.N., Abdul-Latif A. and W.K. Wan Ali
Jurnal Mekanikal, December 2018, 41: 59-73.

Aircraft Trajectory Optimization during Descent Using A *Kriging*-Model-Based-Genetic Algorithm

N. Othman[1,*], M. Kanazaki[2], M. Abd. Wahid[1], S. Mat[1], M.N. Mohd Jaafar[1], W.Z. Wan Omar[1], S. Mansor[1], M.N. Dahalan, M.N. Mohd Nasir, A. Abdul-Latif[1], W.K. Wan Ali[1]

[1]Aeronautics Laboratory, School of Mechanical Engineering, Faculty of Engineering
Universiti Teknologi Malaysia
81310 UTM Johor Bahru
Johor, Malaysia

[2]Graduate School of System Design
Department of Aeronautics and Astronautics
Tokyo Metropolitan University, Hino Campus
6-6 Asahigaoka, 191-0065 Hino City
Tokyo, Japan

ABSTRACT

A time-series flight trajectory technique was developed for use in a civil aircraft during descent. The three-degree-of-freedom (3-DoF) equations of motion were solved via time-series prediction of aerodynamic forces. In the present evaluation, the microburst effect during the descent was considered. The single-objective optimization problem, in which the cost function indicating the trajectory efficiency was minimized, was solved by means of a Kriging model based genetic algorithm (GA) which produces an efficient global optimization process. The optimal trajectory results were compared with those without the microburst condition during the descent. The minimization solution converged well in each case for both conditions plus the differences in flight profiles based on the trajectory history were smaller than those of the solutions before optimization. An analysis of variance and parallel coordinate plot were applied to acquire the quantitative information for the initial condition of descend. The results revealed that the aerodynamic control factors, such as elevators angle and angles of attack, were effective for the minimization of the cost function when microburst is in effective range. According to the visualization results, it was found that a higher airspeed and a larger aerodynamic control by initial elevator were effective for minimizing the cost function when microburst has appeared. It shows that the developed model produced efficient global optimization and can evaluate the aircraft trajectory under the descent situation successfully.

Keywords: *Aerodynamics, efficient global optimization, Kriging model, microburst, trajectory optimization*

1.0 INTRODUCTION

One of the problems in aircrafts' landing processes is unexpected wind [1–2] such as wind shear, gust loading and downburst.

*Corresponding email: norazila@mail.fkm.utm.my

Downburst can be categorized as macroburst and microburst. Specifically, a microburst is a downdraft with winds concentrated in an area less than 4 km in diameter beneath it; and it is typically associated with cumulonimbus clouds [3]. Even though, it is low downdraft winds but it still affects the aircraft motion (pilot control) during take-off and landing at low level altitude (less than 600 m) and make difficult to follow the take-off and landing flight-path. Thus, knowledge for the descent trajectory optimization to safe landed in unexpected wind is a key technique for real advantage in future indicated procedure of air traffic route [4–5]. Instead of previous related works, it is highlighted for the civilian aircraft, and significant of the aerodynamic characteristics influence the performance of aircraft trajectory optimization.

According to a report of National Transportation Safety Board in 1982 [6], a Boeing 727 aircraft operating as Pan American Flight 759 crashed because it did not have sufficient power against a microburst at the time of take-off from the end of the runway. Consequently, the aircraft could not be controlled and it was crashed at a location about 1405 m from the end of the runway horizontally. Therefore, knowledge about techniques against microbursts should be developed sufficiently. Optimum control of angle of attack, pitch angle, and elevator angle has potential to help aircraft designers to solve problems caused by hazardous unexpected wind situations such as microburst. To obtain optimal trajectory and control for avoiding hazardous conditions, time-series aircraft dynamics during landing should be evaluated. Evaluations and designs in consideration of time-series phenomena are important for industrial optimization and design knowledge discoveries in aeronautical engineering. In [7], air traffic was controlled using a model-based speculative virtual machine scheduling algorithm. The shape design optimization under unsteady flow using the ad-joint method was proposed by Siva and Jamesona [8]. However, it remains difficulty to construct global design knowledge by meta-heuristic exploration due to the high computational cost of time series evaluations. Consequently, the related research in aircraft trajectory optimization and finding still continues among researcher until today.

The aim of this research is to indicate the global design knowledge discovery for the aerodynamic control strategy by an efficient global optimization (EGO) [9–13]. The trajectory is estimated using 3-degree-of-freedom (3-DoF) equations of motion (EoM); the aerodynamics are estimated through trajectory evaluations using the United States Air Force (USAF) stability and control data digital computer (DATCOM) [14]. Global optimization is performed by means of EGO which is a *Kriging*-model-based evolutionary algorithm (EA) [9–13]. Using the developed method, the trajectory optimization for a civil aircraft of the scale of a Boeing 777 is considered. The cost function, which indicates the trajectory efficiency profile during the descent of an aircraft, is used. Two cases are compared: one is a trajectory when no microburst occurs, and the other is a trajectory with a microburst happen. An analysis of variance (ANOVA) and a parallel coordinate plot (PCP) are used to discover the knowledge regarding the effects of the input variables.

This paper is organized via four subtopics. The aircraft target model in subtopic two, design methodology and formulation considered here is described in subtopic three, which contain an overview of the proposed method, time-series trajectory optimization (equation of motion and microburst model assumption), and EGO as an optimizer (*Kriging* and genetic algorithms). Finally, the results and discussions are presented in subtopic four. This section contains the trajectory optimization results and a comparison of optimal trajectories with and without a microburst. In addition, knowledge discovery through PCP and ANOVA is discussed. Then, we state the conclusions.

2.0 AIRCRAFT TARGET MODEL

In order to solve the motion of the aircraft, the simulation model called NASA's Common Research Model (CRM) was used. CRM has [15–17] close dimension to the Boeing 777 is used. This reason is the practical aerodynamic database to the real application of descent scenario can be compared. The model is shown in Figure 1 and its specifications are listed in Table 1. In this study, an airframe configuration without an engine is assumed. Instead of simulation model, CRM aircraft is widely used for the experimental wind tunnel study with the specific scale for obtaining the aerodynamic coefficient and performance via experiment. However, in this study the aerodynamics data was compared between DATCOM and CFD only, the experimental data is not in the same conditions based on this study.

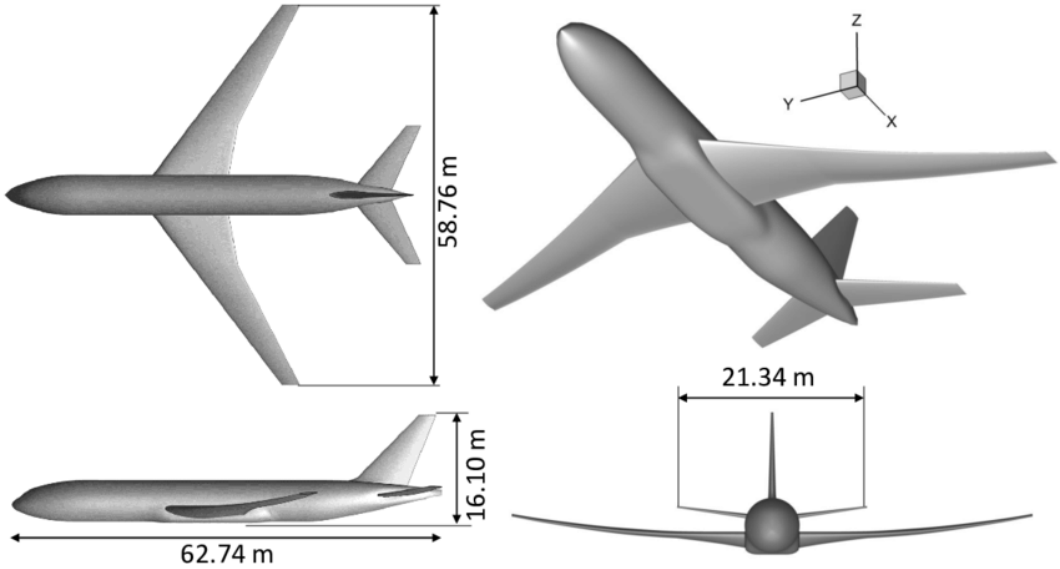

Figure 1: Three views of the aircraft model

Table 1: Specification in DATCOM

Parameter	Dimensions[1]
Swept tapered angle, $\Lambda_{c/4}$	35°
Approximate mass, m	140000.0 kg
Moment of inertia X, I_{xx}	4.8075 kgm^2
Moment of inertia Y, I_{yy}	0.0
Moment of inertia Z, I_{zz}	0.64521 kgm^2

[1]NASA Common Research Model [14–16]

3.0 METHODOLOGY AND FORMULATION

3.1 Design of Experiment

For the design of experiment, three steps are applied. First, *N* samples are selected by space-filling method called Latin hypercube sampling (LHS) [18-19], second, an additional design sample is added, and thirdly the design accuracy is enhanced by constructing a Kriging model based on all $N + 1$ samples. The additional sample is selected using expected improvement (EI) maximization. Genetic algorithm (GA) is applied to solve this maximization problem at this stage. The overall process of this study is shown in Figure 2 [20-25].

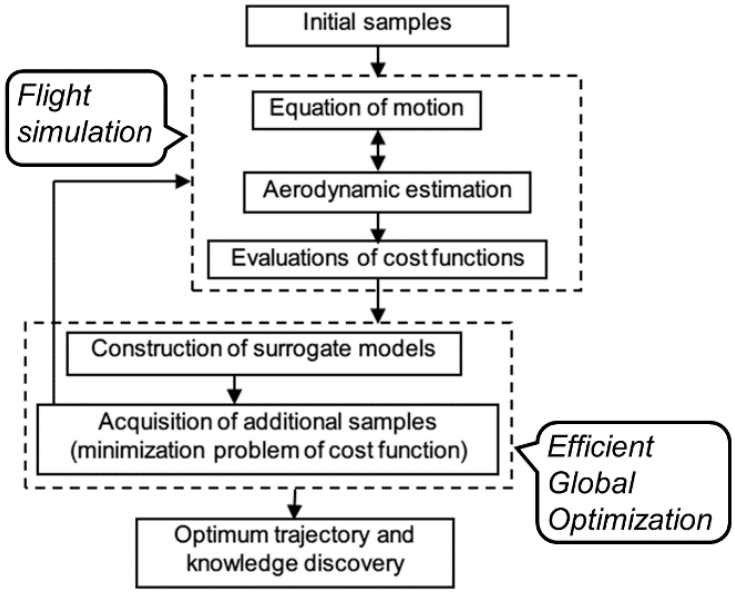

Figure 2: Flowchart of the proposed method; Efficient Global Optimization has two subroutines: flight simulation based aerodynamics estimation and minimization of the cost function

3.2 Problem Definition

The optimal flight profile was obtained in the cases with and without consideration of microbursts. The minimization of the cost function is considered to encounter the microburst. Equation (1) is expressed for the problem definition. The hypothesis condition is shown in Figure 3. The low level altitude is significant contribution microburst phenomena consider the minimization of trajectory function, *J*:

$$Minimize\ J \tag{1}$$

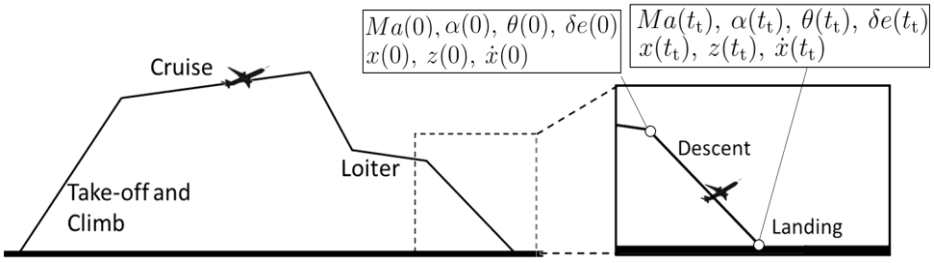

Figure 3: Illustration of the flight profile descent

3.3 *Kriging*-Model-Based Genetic Algorithm as Maximum Likelihood Estimation (MLE)

In mathematical modeling, the process is iterated until the improvement of the objective function becomes negligible. In this study, the *Kriging* method is applied to predict the aerodynamics at unknown flow conditions. To construct the initial database for MLE, efficient *Latin Hypercube* sampling (ELHS) [18-19], is first applied. The $f(\boldsymbol{x})$ is predicted as MLE and can be expressed through the realization of a stochastic process $f(\boldsymbol{x})$ [21-23]:

$$f(\boldsymbol{x}^{(i)}) = \mu + \varepsilon(\boldsymbol{x}) \tag{2}$$

where μ is the global model assumed to be constant, and $\varepsilon(\boldsymbol{x})$ is the local model corresponding to the $\boldsymbol{x}^{(i)}$ design variable for i^{th} sample point. $\varepsilon(\boldsymbol{x})$ is assumed to be a stochastic function as:

$$\mathrm{Con}[\varepsilon(\boldsymbol{x})] = 0 \tag{3}$$

$$\mathrm{Cov}[\varepsilon(\boldsymbol{x}),\ \varepsilon(\boldsymbol{x}')] = \sigma^2 k(\boldsymbol{x}, \boldsymbol{x}') \tag{4}$$

where σ^2 is the process variance and $k(\boldsymbol{x}, \boldsymbol{x}')$ is the correlation function between any two locations $\boldsymbol{x}$ and $\boldsymbol{x}'$. Then, the correlation function is represented as a product of univariate correlation functions for each variable as:

$$k(\boldsymbol{x}, \boldsymbol{x}') = \prod_{k=1}^{n} k(\boldsymbol{x}_i, \boldsymbol{x}_j), \qquad k(\boldsymbol{x}_i, \boldsymbol{x}_j) = \exp\left(-\varphi_i \left|h_i\right|^2\right) \tag{5}$$

where $h_i = \boldsymbol{x}_i - \boldsymbol{x}_j$ and $\varphi_i \geq 0$. This correlation is determined by n hyper-parameters $\boldsymbol{\Theta} = \{\varphi_i, \varphi_i, \ldots\ldots, \varphi_n\}$ for n variables. Using the *Kriging* model [21-23], an attempt is then made to derive a distribution sample over $f(\boldsymbol{x})$ can be expressed as follows:

$$f(\boldsymbol{x}^{(i)}) = \mu + \varepsilon(\boldsymbol{x}^{(i)}), \quad (i = 1, 2, \ldots, n) \tag{6}$$

Thus, μ, σ^2 and $\boldsymbol{\Theta}$ are determined in closed form as:

$$\mu = \left(\mathbf{1}^{\mathrm{T}} \boldsymbol{R}^{-1} \mathbf{1}\right)^{-1} \mathbf{1}^{\mathrm{T}} \boldsymbol{R}^{-1} \boldsymbol{f} \tag{7}$$

$$\sigma^2 = \frac{(\boldsymbol{f} - \mathbf{1}\mu)^{\mathrm{T}} \boldsymbol{R}^{-1} (\boldsymbol{f} - \mathbf{1}\mu)}{n} \tag{8}$$

Here, $\boldsymbol{f} = [f(\boldsymbol{x}^{(1)}), f(\boldsymbol{x}^{(2)}) \ldots\ldots f(\boldsymbol{x}^{(n)})]^{\mathrm{T}}$, $\boldsymbol{R}$ is a matrix whose (i, j) for n sampling entry is $k(x^{(i)}, x^{(j)})$, and $\mathbf{1}$ is the n-dimensional vector ($[1, 1, \ldots, 1]^{\mathrm{T}}$). The variable of MLE, which represents the probability density distribution (PDF), can be expressed as:

$$\mathrm{MLE}\left(\mu, \sigma^2\right) = \ln\left(\mathrm{PDF}\left(\boldsymbol{f} \left| \boldsymbol{x}^{(1)}, \boldsymbol{x}^{(2)}, \ldots, \boldsymbol{x}^{(n)} \right.\right)\right) \tag{9}$$

Genetic algorithm (GA) is used to search for the values of $\boldsymbol{\Theta}$ by solving the MLE. The final approximation value $\boldsymbol{f}$ using the *Kriging* method can be expressed as follows:

$$f(\boldsymbol{x}) = \mu + \boldsymbol{r}^{\mathrm{T}}(\boldsymbol{x}) \boldsymbol{R}^{-1} (\boldsymbol{f} - \mathbf{1}\mu) \tag{10}$$

In ordinary *Kriging*, $\boldsymbol{r}(\boldsymbol{x})$ is an n dimensional vector whose i^{th} element is $k(\boldsymbol{x}, \boldsymbol{x}^{(i)})$, $\boldsymbol{R}$ is the correlation matrix, $\boldsymbol{R}^{-1}$ is the inverse of matrix $\boldsymbol{R}$, Equation (10) is an estimate of $f(\boldsymbol{x})$ at any location $\boldsymbol{x}$ by interpolating the sample points with the exact values of $f(\boldsymbol{x})$. A smaller distance between $\boldsymbol{x}$ and the sample points yields a less uncertain and more accurate *Kriging* prediction $f(\boldsymbol{x})$.

In order to improve the samples of the aerodynamic model and acquire optimum solutions, the expected improvement (*EI*) was used. *EI* is defined as the expected value of how much an objective function can be improved for maximization and minimization by the *EI* maximum points due to the *Kriging* surrogate model. *EI* can be used for improving the database and determining the global optimum points. The *EI* can be written as:

$$EI[f(\boldsymbol{x})_{\min/\max}] = \int_{-\infty}^{f_{\text{ref}}} (f_{\text{ref}} - f)\phi(f)df \tag{11}$$

where f is the approximated model with MLE variables error, f_{ref} is the maximum or minimum point and $\phi(f)$ is the probability density distribution function as shown in Equation (9). To solve this problem, *EI*s were used to minimize the trajectory function, J from Equation (1) [21]. The subroutine in EGO and related to GA [21-23] as a solver for the given problem is defined as:

$$J = \phi\left[x(t_f)\right] + \int_{t_0}^{t_f} L[x(t), u(t), W(t), t]dt \tag{12}$$

subject to:

$$\dot{x} = f\left(x(t), u(t), W(t), t\right)$$
$$x(t_0) = x_0$$
$$\text{For all } t \in [t_0, t_f]$$

where, $x = [A]x + [B]\eta + [C]\xi$ is containing state matrix A, control spaces matrix B and microburst disturbance matrix C, $\phi[x(t_f)]$ is from the intended flight-path which $x(t_f)$ comprises the vector of the final state perturbation from the nominal flight condition and flight path. The matrix of $\phi[x(t_f)]$ is the solution of the discrete-time algebraic equation involving the sample-data linearization of the 3-DoF equations of motion and involving the cost function integrand, L that describes the non-linear longitudinal motions of an aircraft in condition of microburst. Then, L=[x, u, t] can be defined as:

$$L[x, u, t] = \left\{2\left[(z_t - z_0)\cos\alpha_0 - (x_t - x_0)\sin\alpha_0\right]^2 + 0.04\left[\delta e_t - \delta e_0\right]^2\right\} \tag{13}$$

L describes the state and control inequalities that must be enforced for the optimal solution to make physical and practical sense. Based on Figure 2, the input variables for the optimization problem, including the initial and final conditions, $Ma(0)$, $\alpha(0)$, $\theta(0)$, $\delta e(0)$, $x(0)$, $z(0)$, $\dot{x}(0)$, $Ma(t_f)$, $\alpha(t_f)$, $\theta(t_f)$, $\delta e(t_f)$, $x(t_f)$, $z(t_f)$, $\dot{x}(t_f)$, are defined to solve Equation (1). In order to solve this problem, we set $x(0)$ = 0.0 [m], $x(t_f)$ = 3000.0 [m], $z(0)$ = 600.0 [m], $z(t_f)$ = 0.0 [m], $\dot{x}(0)$ = 160.0 [m/s], $\dot{x}(t_f)$ = 0.0 [m/s], $Ma(t_f)$ = 0.0, $\alpha(t_f)$ = 2.0 [º] and $\theta(t_f)$ = 0.0 [º]. Here, t = 0.0 s is the time when the aircraft starts and t_f is its final landing time. $Ma(0)$, $\alpha(0)$, $\theta(0)$ and $\delta e(0)$ are considered as the suitable design variables and their ranges based on the previous study were set as [4]:

$$0.0 \leq Ma(0) \leq 0.3$$

$$-2.0 \leq \alpha(0) \leq 16.0$$

$$0.0 \leq \theta(0) \leq 12.0$$

$$-8.0 \leq \delta e(0) \leq 8.0$$

The time variation of $\delta e(t)$ was decided at several segments (sampling times) during the flight along with minimizing the cost function for the design variables - $Ma(0)$, $\alpha(0)$, $\theta(0)$ and $\delta e(0)$.

3.5 Time-Series Trajectory Evaluation

Trajectory evaluation is based on equations of motion (EoMs) by acquiring the time-series aerodynamic forces which is matrix *A* as state condition of aircraft. It is estimated by the nonlinear 3-DoF EoMs. From this relation, the aerodynamics derivatives can be calculated via DATCOM. In this analysis, the assumption flight trajectory with no engine thrust variation effect is considered because we use the CFD model based on NASA Common Research Model (CRM) [15–17]. The analysis also includes a microburst term expressed as in Equation (14):

$$\begin{aligned} \frac{d^2x_b}{dt^2} &= \frac{X}{m} - g\sin\theta - \frac{d\theta}{dt}\left(V\sin\alpha + W_{Z_b}\right) - \dot{W}_{x_b} \\ \frac{d^2z_b}{dt^2} &= \frac{Z}{m} + g\cos\theta + \frac{d\theta}{dt}\left(V\cos\alpha + W_{x_b}\right) - \dot{W}_{z_b} \\ \frac{d^2\theta}{dt^2} &= \frac{M}{I_{yy}} \end{aligned} \tag{14}$$

The force components, *X* and *Z* consisting of the aerodynamic lift and drag effects can be expressed as:

$$X = -D\cos\alpha + L\sin\alpha \text{ and } Z = -D\sin\alpha - L\cos\alpha \tag{15}$$

x_b and z_b are referred to as the horizontal positive upward and tangent of x_b positive downward direction of body coordinates. θ is the pitch angle, ϕ is the flight path angle, α is the angle of attack, M is the pitching moment, and I_{yy} is the moment of inertia with respec to the *y* axis. m is the mass of the aircraft and g is its gravitational acceleration. W_x and W_z are the effective microburst forces in the *x*-direction and *z*-direction, respectively and their reference to the earth as inertial reference [22].

The microburst model W_{Z_E}, W_{X_E} are assumed in the inertial frame of reference and converted into the body-axis frame as:

$$\begin{bmatrix} W_{X_b} \\ W_{Z_b} \end{bmatrix} = \begin{bmatrix} \cos\theta & -\sin\theta \\ \sin\theta & \cos\theta \end{bmatrix} \begin{bmatrix} W_{X_E} \\ W_{Z_E} \end{bmatrix} \tag{16}$$

Here, the influence of $\dot{\alpha}$ on $\dot{W}_{x_b}$ and $\dot{W}_{z_b}$ in Equation (16) are assumed to be negligible because it is too small and remain constant due to the low level altitude. The effect of the microburst is included in the lift and the drag as follows:

$$\begin{aligned} L &= 1/2\rho(V\cos\alpha + Wx_b)^2 + (V\sin\alpha + Wz_b)^2 S_{ref} C_L \\ D &= 1/2\rho(V\cos\alpha + Wx_b)^2 + (V\sin\alpha + Wz_b)^2 S_{ref} C_D \\ M &= 1/2\rho(V\cos\alpha + Wx_b)^2 + (V\sin\alpha + Wz_b)^2 S_{ref} c_{ref} C_m \end{aligned} \tag{17}$$

The assumption is based on a pilot-in-the-loop simulation, which is a considerably simple wind model [24]. This model consists of constant outflow outside the microburst radius and constant slope headwind and tailwind shear across the diameter of the microburst.

3.5 Aerodynamics Model

The force components, force *X*, normal force *Z* and pitching moment *M* are required to be estimated with time variation effect such as the derivatives from pitch rate, *q*, elevator angle, δe while solving the EoMs as shown in Equation (15) [26-27]. For the half span model geometry data and flight condition, the aerodynamic derivatives can be predicted. In this study, $Cz_q = \partial Cz/\partial q$, $Cx_\alpha = \partial Cx/\partial \alpha$, $Cm_q = \partial Cm/\partial q$, and $Cm_\alpha = \partial Cm/\partial \alpha$ are determine via USAF stability and control DATCOM [14]. Based on the prediction components of aerodynamic derivatives, then the aerodynamic model coefficients are evaluated as shown in Equation (18) [27].

$$\begin{aligned} Cz &= Cz_0 + Cz_\alpha \alpha + Cz_q q + Cz_{\delta e}.\delta e \\ Cx &= Cx_0 + Cx_\alpha \alpha + Cx_q q + Cx_{\delta e}.\delta e \\ Cm &= Cm_0 + Cm_\alpha \alpha + Cm_q q + Cm_{\delta e}.\delta e \end{aligned} \tag{18}$$

3.6 Microburst Model Assumptions

The assumption of microburst model is made in this study because it is minor downdraft wind and pushing aircraft to the ground suddenly. In this condition, it can cause loss thrust to the aircraft while landing. W_{x_E} and W_{y_E} in Equations (19) and (20) are used with the same magnitude of the microburst model as shown in Figure 5. W_{x_E} can be expressed as:

$$W_{x_E} = W_{y_E} = \frac{2W_{X\max}(x - x_{\text{mbo}})}{x_{\text{mbl}}} \tag{19}$$

where x_{mbo} is the started source position of the microburst, x_{mb1} is the radius of the microburst, and $W_{X\max}$ is the maximum value of the horizontal microburst wind reference to the earth axis. As a final point, after a microburst exits the effective range, a steady tail wind appears at W_{z_E} and is expressed as:

$$W_{z_E} = \frac{-4W_{X\max}}{x_{\text{mbl}}} h \tag{20}$$

Note that the negative sign explains the microburst employs force in the downward direction, as *h* is the altitude to the downward of earth. In this study, the limitation of the horizontal wind position is assumed as a constant extends to infinite distance.

4.0 RESULTS AND DISCUSSION

4.1 Aerodynamics Results

Aerodynamic forces obtained by Equation (18) using DATCOM were compared with the results by the computational fluid dynamics (CFD) for the validation. The compressible *Navier-Stokes* equation was solved to obtain the CFD results. Figure 4 shows comparisons of C_X, C_Z and C_M. According to these figures, results by DATCOM were almost in agreement with the CFD counterpart at low angles of attack. The reason is at a low angle of attack, the instability flow slightly not occuring at the transonic speeds and comparison agrees well between DATCOM and CFD findings. The CFD approach indicates close value to the DATCOM results for one specific calculation of one angle of attack and *Mach* number. Comparison of the derivatives can be referred to Psiaki and Stengel for jet transport type of aircraft [4]. For the analysis at low angle of attack, the

aerodynamic forces based on DATCOM were used in the following sub-sections to reduce the time computation by CFD.

4.2 Trajectory Optimization Results

Figure 5 shows the optimization history, including the additional sampling process, by EGO with/without consideration of microbursts. EGO process was started with 76 initial samples and 43 samples of additional designs were obtained by *EI*s maximization. To decide the time variation of the $\delta e(t)$, 100 segments were set during the landing approach. According to Figure 5, many additional samples could be obtained around the minimum *J*.

In addition, Figure 6 shows the comparison of the descent trajectories which perform the maximum and minimum *J*. Based on the conventional descent approach, the descent followed a linear trajectory, for which the fuel consumption was effective during the phase when there are no disturbances. Then, for any disturbances, the trajectory must follow the descent approach flight path linearly. As shown in Figure 6(a), when a microburst occurs, the trajectory *z*, which achieves the maximum *J* is less affected than the trajectory without the microburst. In addition, *z* of the aircraft decreases owing to the downward wind after 150.0 s. In the case of maximum *J,* α decreases suddenly in cases with and without microburst at approximately 180.0 s as shown in Figure 6(b), as the time variation of δe as shown in Figure 6(c) is not optimized in each case. On the other hand, according to Figure 6(a), whose trajectory achieved the minimum *J*, the trajectory obtained considering the microburst effect is closer to that obtained without microburst. This figure also suggests that δe of Figure 6(c) must be changed in a smooth manner to reduce *J*. It was also observed that, during descent, δe must be high with microburst compared to that without microburst. The angle, α should be reduced as shown in Figure 6(b) of the minimum *J* case, during descent with microburst to recover from sudden unexpected vertical wind owing to the microburst condition.

4.3 Analysis of Variance ANOVA

ANOVA is employed to investigate the effects of the design variables on the objective functions. It is based on the *Kriging*-model that shows the contributions of designed variables to target functions. Figure 7 shows the contribution ratio of designed variables for the minimization of *J*. Figures 7(a) and (b) shows the ANOVA results, and it suggests that the main effect of δe (0), as well as the two-way interaction of δe (0) and α (0), are highly effective. To maintain a smooth decent, aerodynamic control factors, α and δe are important. On the other hand, the significant value of $Ma(0)$ could not be observed. For further understanding, the timely variation of $Ma(t)$, $\alpha(t)$, $\theta(t)$, and δe (t) using PCP is discussed in the next sub-section.

4.4 Design Space Evaluation by PCP

In this study, the statistical visualization technique is used to show the relationship of the design variables and target function simultaneously on the same graph called parallel coordinate plot (PCP). It was employed to transform high-dimensional data into two-dimensional graphs [28 - 29]. In order to draw the PCP, the normalization of the attribute values in the design problem, such as design variables, objective functions and constraint value wa carried out. Figure 8 shows the comparison of the PCP visualization for cases with and without the microburst where the time-series $Ma(150)$, $Ma(250)$, $\alpha(150)$, $\alpha(250)$, $\theta(150)$, $\theta(250)$, δe (150), and δe (250), are the variables at the starting and ending time (t =150.0 s and 250.0 s) of the microburst effective time, respectively. They were explored with respect to *J*, as well as the designed variables ($Ma(0)$, $\alpha(0)$, $\theta(0)$, and δe (0)) to observe the global trends. Figures 8(a) and (b) show the results obtained when the microburst was not considered while Figures 8(c) and (d) illustrate the results obtained when the microburst was presence. On the other hand, the possible ranges of these

parameters that determine the trajectory were narrowed for obtaining the optimum trajectory after 100.0 s, i.e., $Ma(t)$ was approximately set to 0.15 to 0.10, $\alpha(t)$ was set to approximately 10.0º to 1.0º, $\theta(t)$ was set to about 15.0º to 8.0º and $\delta e(t)$ was approximately set to -6.0º to -2.0º.

This result suggests that a robust trajectory can be obtained using the proposed design procedure. The design was performed with several initial flight conditions for landing. In addition, based on Figure 8(b), it can be observed that the time variation of $Ma(t)$, $\alpha(t)$, $\theta(t)$, and $\delta e(t)$ in the microburst effective time (from t = 150.0 s to 250.0 s) for without microburst are approximately 0.14 – 0.18 to 0.08, 5.0º to 4.0 – 5.0º, 8.5–10.0º to 7.0 – 8.0º and -4.0º to -2.0º, respectively [3].

From Figure 8(d), it can be observed that the time variation in $Ma(t)$, $\alpha(t)$, $\theta(t)$, and $\delta e(t)$ in the microburst effective time are approximately 0.14 – 0.18 to 0.10, 6.0º to 1.0, 2.0º, 7.0 – 10.0º to 7.0 – 8.0º, and -6.0º to -1.0º, respectively [3]. Consequently, the reduction in $Ma(t)$ is smaller in order to maintain suitable lift against the microburst to achieve minimum J when microburst is effective than that when microburst is not effective. In fact, according to Figure 9(b), the altitude z was maintained when microburst is effective, while z in Figure 9(a) rapidly decreased. In addition, the reduction in $\alpha(t)$ is larger when microburst is effective. In this case, $\theta(t)$ is almost constant at t = 150.0 s – 250.0 s because the increment in $\delta e(t)$ is larger when microburst is effective than that when microburst is not effective, as shown in Figure 10(d). It suggests that a larger control by appropriate setting of $\delta e(t)$ is required against a larger variation of $\alpha(t)$ to maintain $\theta(t)$ constant and minimize J.

4.5 Validation of Trajectory Evaluation

The optimum trajectory in case with the microburst effect was compared with other related studies to validate the reliability of present approach. Figure 9 shows the comparison between the trajectory obtained in this study and two optimization results [4 – 5]. Equation (1) was solved using the same boundary conditions as those used in [4 – 5], $Ma(0)$ = 0.11, $\alpha(0)$ = 3.0º, $\theta(0)$ = 2.0º, $\delta e(0)$ = −1.0º, $x(0)$ = 0.0 m, $h(0)$ = 182.89 m (600.0 ft), $\dot{x}(0)$ =100.0 m/s, $Ma(t_f)$ = 0.0, $\alpha(t_f)$ = −1.0º, $\theta(t_f)$ = 0.0º, $\delta e(t_f)$ = 0.0◦, $x(t_f)$ = 3657.6 m (12000.0 ft), $z(t_f)$ = 0.0 m, $\dot{x}(t_f)$ = 0.0 m/s. According to Figure 9, it was found that our optimal trajectory is in the range of other studies. In addition, the proposed study has produced trajectories close to the desired flight path that can maintain a constant altitude more convenient for the passengers [4]. This is because the trajectory is close to the straight line suggested from the specified glide path slope of tan(-3.0º) [4]. In particular, the practical applications of these results are discussed in [4] and thus, the obtained results represent an acceptable trajectory for the real aircraft.

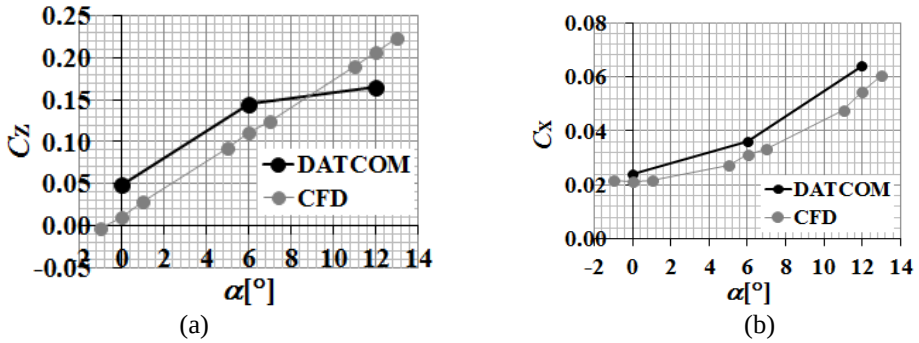

(a) (b)

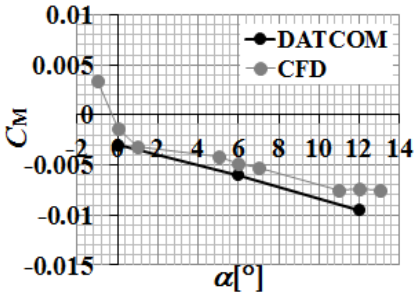

(c)

Figure 4: Comparison of results using DATCOM and CFD of the aerodynamic forces and pitching moment coefficients using $Ma = 0.1$ and varying α for (a) C_Z, (b) C_X and (c) C_M

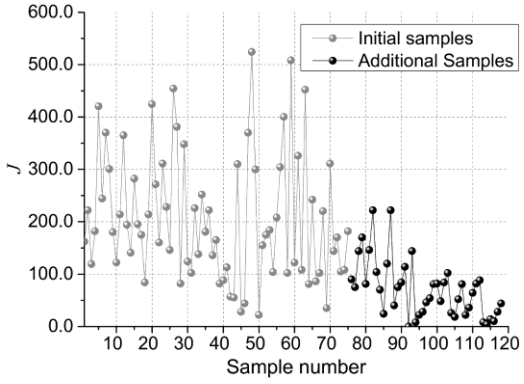

(a)

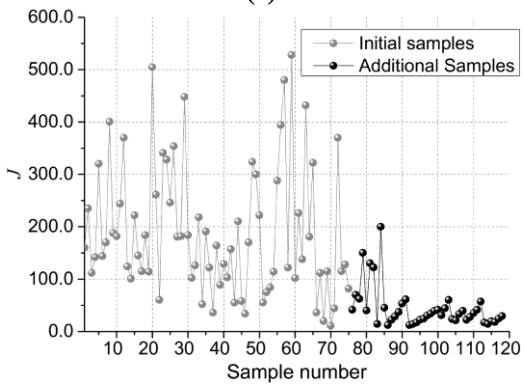

(b)

Figure 5: Histories of design exploration using EGO (a) without microburst and (b) with microburst

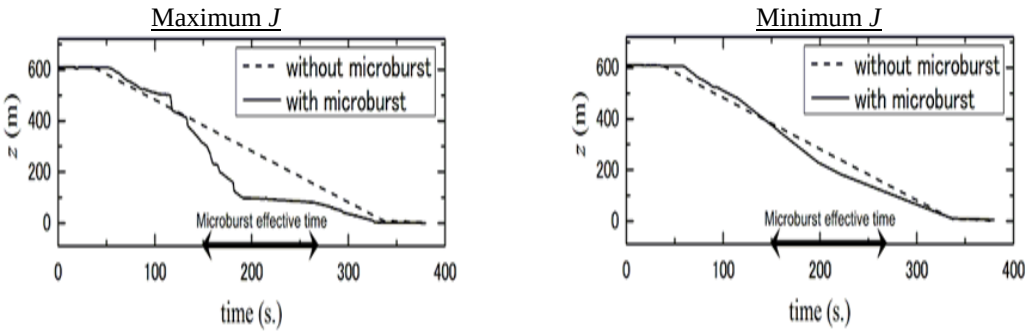

(a)

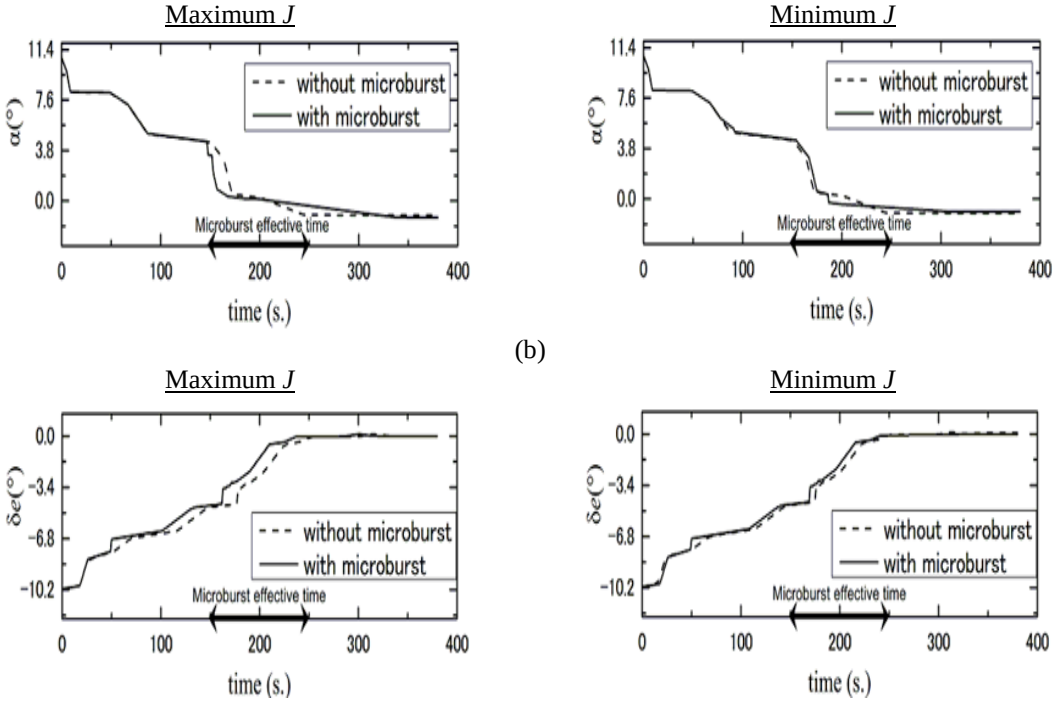

(b)

(c)

Figure 6: Comparison of trajectory histories based on: (a) Altitude (b) Angle of attack and (c) Elevator angle as input variables

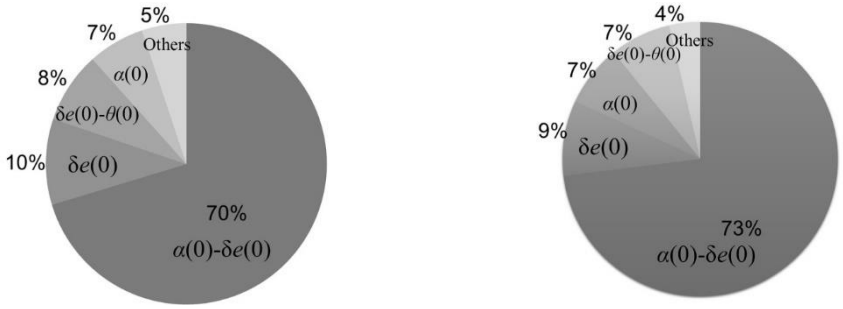

(a) (b)

Figure 7: Comparison results of ANOVA for the case of minimum *J*: (a) without microburst (b) with microburst

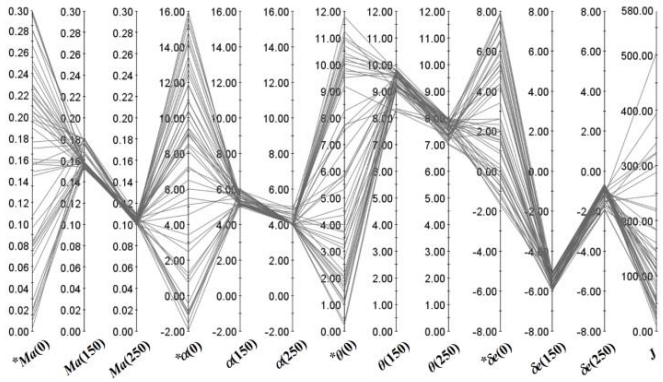

(a)

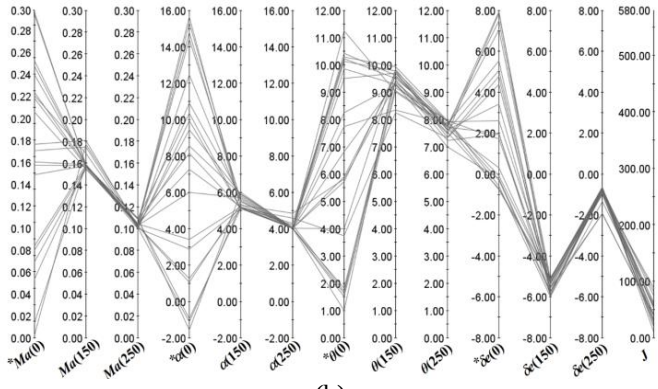

(b)

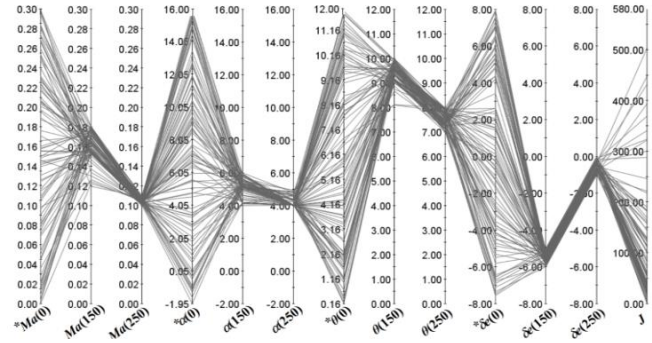

(c)

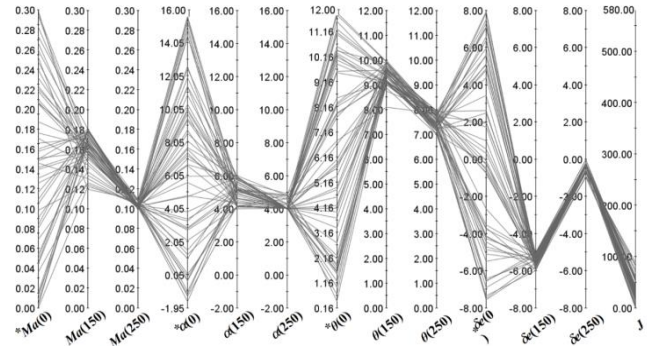

(d)

Figure 8: Comparison of the design results visualization by PCP. Variables with "*" are designed variables. (a) All solutions obtained without microburst, (b) solutions sorted by *J* for the case without microburst, (c) all solutions obtained with microburst and (d) solutions sorted by *J* for the case with microburst.

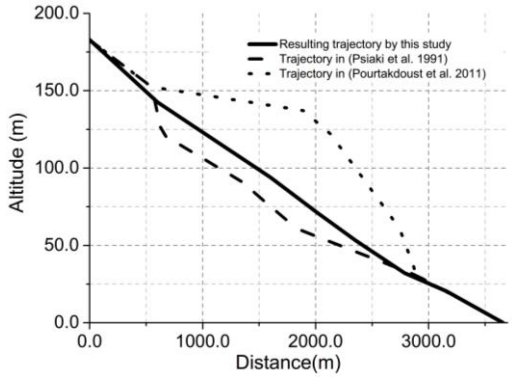

Figure 9: Comparison of the trajectory (*z*-altitude versus *x*-distance) between current simulation and other approaches

5.0 CONCLUSIONS

The time-series trajectory evaluation for the optimization descent of an airplane with and without microbursts was achieved using the global optimization technique. The 3-DoF equations of motion were solved considering the time-series aerodynamics. The optimization problem considered in this study aimed to minimize the cost function defined to improve the descent trajectory efficiency. The optimization problem was solved using an efficient global optimization technique through a genetic algorithm based on a *Kriging* model. The functional analysis of variance based on the *Kriging* model was also applied to reveal the relationships of the several influential key variables. The PCP was also employed to visualize the design problem, including the time-variance of designed variables.

The results showed that the trajectory optimization obtained using the developed method, for the cases with and without microburst with additional samples achieves lower cost functions. On comparing the resulting trajectory, the variations in altitudes and angles of attack were maintained with optimal time variation of the elevator angle. During descent, a greater elevator angle was used when the microburst effect was considered than that when the microburst effect was not considered. The variance results revealed that the aerodynamic control factors, such as elevator angles and angles of attack were effective. According to PCP plot visualization, it was found that a higher airspeed and larger aerodynamic control were effective for minimizing the cost function with microburst than that without microburst. The proposed method can be applied to both conventional and unconventional aircrafts, such as blended wing body type concept, which require knowledge regarding safety and efficient flight through microbursts. A part of that, the proposed method is targeted to apply widely for the development of new aircrafts and development of new flight management techniques against hazardous situations, under the condition that the demand for civil aircraft will increase.

ACKNOWLEDGMENTS

The author would like to express deep appreciation for the research funded by the Asian Human Resources Fund (AHRF) obtained from the Tokyo Metropolitan Government to the Tokyo Metropolitan University (TMU). Special thanks to the Aeronautics Laboratory, School of Mechanical Engineering, Universiti Teknologi Malaysia (UTM) and the Malaysian Ministry of Education (MOE) for providing the grants - special academic fund (PAS No: 02K81) and FRGS/1/2018/TK09/UTM/02/4, respectively throughout this study.

REFERENCES

1. Fujita T., 1990. Downbursts: Meteorological Features and Wind Field Characteristics, *Journal of Wind Engineering and Industrial Aerodynamics*, 36(1):75–86.
2. Vicroy D.D., 1992. Assessment of Microburst Models for Downdraft Estimation, *Journal of Aircraft*, 20(6):1043–1048.
3. Pourtakdoust S.H., Kiani M. and Hassanpour A., 2011. Optimal Trajectory Planning for Flight through Microburst Wind Shear, *Aerospace Science and Technology*, 15(7): 567–576.
4. Psiaki M.L. and Stengel R.F., 1991. Optimal Aircraft Performance During Microburst Encounter, *Journal of Guidance, Control and Dynamics*, 12(4):155–161.
5. Psiaki M.L. and Stengel R.F., 1986. Optimal Flight Paths Through Microburst Wind Profiles, *Journal of Aircraft*, 23(8):629–635.
6. National Transportation Safety Board (NTSB), 1982. *Aircraft Accident Report*, PB83-910402.

7. Lee B.J. and Lioua M.S., 1990. Unsteady Adjoint Approach for Design Optimization of Flapping Airfoils, *AIAA Journal*, 36(1):75–86.
8. Siva, S. K., and Jamesona, A. 2000. Optimum Shape Design for Unsteady Flows with Time-Accurate Continuous and Discrete Adjoint Method, *AIAA Journal*, 45(7):1478–1491.
9. Donald, R. J., Matthias, S., and William, W. J. 1998. Efficient Global Optimization of Expensive Black-Box Function, *Journal of Global Optimization*, 13:455–492.
10. Pehlivanoglu, V. V., and Yagiz, B. 2005. Aerodynamic Design Prediction Using Surrogate-Based Modeling in Genetic Algorithm Architecture, *Aerospace Science and Technology*, 42(2):413–420.
11. Jeong S., Murayama, M., and Yamamoto, K. 2005. Efficient Optimization Design Method Using Kriging Model, *Journal of Aircraft*, 42(2):413–420.
12 Kanazaki, M., and Jeong, S. 2007. High-Lift Airfoil Design Using Kriging Based MOGA and Data Mining, *Korea Society for Aeronautical and Space Sciences International Journal*, 8(2):28–36.
13. Kanazaki, M., Obayashi, S., and Nakahashi, K. 2004. Exhaust Manifold Design With Tapered Pipes Using Divided Range MOGA, *Engineering Optimization*, 36(2):149–164.
14. Fink, R.D. 1978. *USAF Stability and Control DATCOM, Flight Control Division*. AFWAL-TR-83-3048.
15. Koga S., Kohzai M., Ueno M., Nakakita K. and Sudani N., 2013. Analysis of NASA Common Research Model Dynamic Data In JAXA Wind Tunnel Tests, *AIAA Journal*, 1–11.
16. Hashimoto A., Murakami K., Aoyama T., Yamamoto K. and Murayama M., 2010. Drag Prediction on NASA CRM Using Automatic Hexahedra Grid Generation Method, *48th AIAA Aerospace Sciences Meeting including The New Horizons Forum and Aerospace Exposition*, Orlando, Florida, AIAA 2010-1417.
17. John C.V., Mark A.D., Melissa S.R. and Richard A.W., 2008. Development of A Common Research Model for Applied CFD Validation Studies, *26th AIAA Applied Aerodynamic Conference, Guidance, Navigation, and Control and Co-located Conferences*, Honolulu, Hawaii, AIAA 2008-6919.
18. Ales F., 1992. An Efficient Sampling Scheme: Updated Latin Hypercube Sampling, *Probabilistic Engineering Mechanics*, 7(2):123–130.
19. Nestor V.Q., Raphael T.H., Shyy W., Goel T., Vaidyanathan R., Tucker P.K., 2005. Surrogate-Based Analysis and Optimization, *Progress in Aerospace Sciences*, 41(1):1–28.
20. Mulgund S.M. and Stengel R.F., 1993. Optimal Recovery from Microburst Wind Shear, *Journal of Guidance, Control and Dynamics*, 16(6):1010–1017.
21. Kanazaki M. and Othman N., 2016. Time-Series Optimization Methodology and Knowledge Discovery of Descend Trajectory for Civil Aircraft, *Evolutionary Computation (CEC), IEEE Congress.* 24-26 July 2016. Vancouver, BC, Canada.
22. Lian Y., Oyama A. and Liou M.S., 2010. Progress in Design Optimization Using Evolutionary Algorithms for Aerodynamic Problems, *Progress in Aerospace Sciences*. 46:199–223.
23. Shimoyama K., Jeong S. and Obayashi S., 2015. Kriging-Surrogate–Based Optimization Considering Expected Hypervolume Improvement in Non-Constrained Many–Objective Test Problems, *IEEE Congress on Evolutionary Computation*, Cancun, Mexico, 2015:658–665.
24. Lee K.H. and Park F.J., 2006. A Global Robust Optimization Using Kriging Based Approximation Model, *JSME International Journal Series* C, 49(3):779–788.
26. Hinton D.A., 1989. Piloted-Simulation Evaluation of Escape Guidance for Microburst Wind Shear Encounters, *NASA Technical Paper*, NASA Langley Research Center, 233665 (5225):1–13.
27. Ghoreyshi M., Badcock K.J., Ronch A., Da Marques S., Swift A. and Ames N., 2011. Framework for Establishing Limits of Tabular Aerodynamic Models For Flight Dynamics Analysis, *Journal of Aircraft*, 48(1):42–55.
28. Inselberg A., 1985. The Plane with Parallel Coordinates, *The Visual Computer*, 1(2):69–91.
29. Wegman E.J., 1990. Hyperdimensional Data Analysis Using Parallel Coordinates, *Journal of the American Statistical Association*, 85(411):664-675.